Experimental and Theoretical Thermal Performance of Double Pass Solar Air Heater with Porous Media

M. YAHYA, K. SOPIAN, M. Y. THEERAN, M. Y. OTHMAN, M. A. ALGHOUL, M. HAFIDZ and A. ZAHARIM
Solar Energy Research Institute
Universiti Kebangsaan Malaysia
43600 Bangi Selangor
MALAYSIA

Abstract: - A theoretical model has been developed to predict the thermal performance of double pass solar air heater with porous media. It is composed of five-coupled unsteady nonlinear partial differential equations which are solved by using numerical scheme. Instead of solving the simultaneous equations for temperature at each element, a matrix inversion was employed. An experimental setup has been designed and constructed. The thermal performance testing was conducted indoor by using a solar simulator. Comparisons of the theoretical and experimental results have been conducted and it was found the theoretical and the experimental results show a good agreement.

Key-Words: Double pass solar collector, iteration, numerical, porous media, and solar radiation.

1 Introduction

There are numerous works on solar air heaters been conducted for use in space heating and thermal industrial processes. In tropical climates, solar air heater can be a fully or a partially employed to supply hot air such as to dryer. Satchunanathan and Deneonarine [1], Satchunanathan and persad [2], Mohamad [3], performed the experiments and conducted analytical studies involving double pass solar air heater. They concluded according to their experimental and analytical results, that double pass design with flow between two glass covers and under the absorber plate, had a thermal efficiency about 10% higher than the single pass design. In a series of investigations conducted at the National University of Malaysia. Much experimental data were obtained with regards to the performance of double pass solar air heater with porous media. The theoretical models were early presented by Suprianto [4], Elradi [5] and Ooi [6]. Their investigations considered the steady state heat balance equations by using where the Hottel-Whilier-Bliss equation or close loops method. Ong [7] presented a simple matrix inverse method of solution which obviated the need for complex algebraic manipulation of energy equations.

Solar radiation and other meteorological conditions always varied. The further study of theoretical model for solar collector in transient stated could be more significant to predict the out door performance of the solar collector.

2 Objectives

This paper presents the results of the theoretical and experimental studies on the thermal performance of double pass solar air heater with porous media. Matrix inverse method of solution was employed using a standard sub-routine computer program. Since the experiments set up is subjected to meteorological data, this paper proposes to modify into a transient one, which also takes into account the conduction heat transfer. Numerical scheme has been proposed to solve five coupled unsteady including nonlinear partial differential equations. The model would able to predict thermal distribution within collector, and effect of any change of input such as solar radiation and ambient temperature.

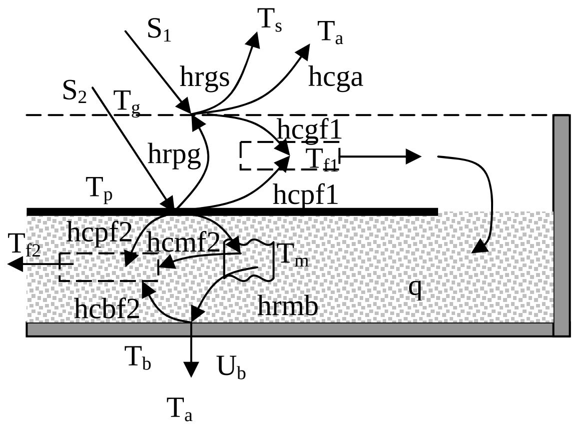

Fig. 1 Schematic diagram of double pass solar air heater with porous media.

3 Analysis Theory

Design of double pass solar air heater with porous media was shown in figure 1. Air flow from upper channel and return back through lower channel. Steel wool as a porous media is packed in the lower channel. The Porous media which has covered the bottom plate was considered beside the bottom plate when expressing the thermal equilibrium. The glass cover absorbed some portion of the solar radiation which fall on the collector and the rest was absorbed by the absorber plate. Refer to the above figure. The following transient equations are obtained:

Heat balance through glass cover;

$$Q_{rgs} + Q_{cga} + Q_{cgf1} + Q_{\theta Tg} = S_1 + Q_{rpg}$$

$$h_{rgs}(T_g - T_s) + h_{cga}(T_g - T_a) + h_{cgf1}(T_g - T_{f1}) + m_g c_g (dT/dt)_g = S_1 + h_{rpg}(T_p - T_g) \quad (1)$$

At the upper stream for air flowing between glass cover and absorber plate;

$$(m_{ft}c/w)(dT/dx) + Q_{\theta Tf1} = Q_{gf} + Q_{pf}$$

$$(m_{ft}c/w)(dT/dx)_{f1} + mc_{f1}(dT/dt)_{f1} = h_{cgf1}(T_g - T_{f1}) + h_{cpf1}(T_p - T_{f1}) \quad (2)$$

Heat balance through absorber plate;

$$Q_{pg} + Q_{pf1} + Q_{pf2} + Q_{pq} + Q_{\theta Tg} = S_2$$

$$Q_{pR} = Q_{pb}$$

$$h_{pg}(T_p - T_g) + h_{pf1}(T_p - T_{f1}) + h_{pf2}(T_p - T_{f2}) + h_{pR}(T_p - T_R) + mc_p(dT/dt)_p + k_p\delta_p(d^2T_p/dx^2) = S_2 \quad (3)$$

Heat balance at the second stream was derived without forgetting the air flow backward through lower channel, as shown below;

$$(m_{ft2}c/w)(-dT/dx)_2 + Q_{\theta Tg} = Q_{pf2} + Q_{bf2}$$

$$(m_{ft2}c/w)(-dT/dx)_{f2} + mc_{f2}(dT/dt)_{f2} = h_{cpf2}(T_p - T_{f2}) + h_{cbf2}(T_b - T_{f2}) \quad (4)$$

Heat balance through bottom plate;

$$Q_{ba} + Q_{\theta Tg} = Q_{bf2} + Q_{bp}$$

$$U_b(T_b - T_a) + mc_b(dT/dt)_b + k_b\delta_b(d^2T_b/dx^2) = h_{bf2}(T_{f2} - T_b) + h_{bp}(T_p - T_b) \quad (5)$$

$$S_1 = \alpha_g S \quad (6)$$

$$S_2 = \tau_g\alpha_p S \quad (7)$$

Those first five couple unsteady state equations including nonlinear partial differential equations has been simplified by Elrady [5] by assuming that the air and porous media is in equilibrium i.e. the temperature of porous media is equal to the temperature of the zone air. Supranto [4] has made more simplifications by assuming that the air, porous media and the bottom plate are in thermal equilibrium. Ong [7] considered the surface temperature of the walls surrounding the air stream is uniform whereas the air temperature is assumed to vary linearly along the collector. From his observations he found that these assumptions are valid for short collectors only. In close loop method, done by Sopian et al [8], Garg et al [9], they have shown that the temperature was varied exponentially along the collector. Five unsteady state simultaneous equations can be solved by numerical method. First order and second order differentiation equations are defined as follow;

$$dT/dt) = (T_m - T_{(m-1)})/dt\,; \quad (8)$$

$$(dT/dx)_{f1} = (T_{f1n} - T_{f1(n-1)})/dx,$$

$$(dT/dx)_{f2} = (T_{f2(n+1)} - T_{f2(n)})/dx; \quad (9)$$

$$(d^2T/dx^2) = (T_{(n+1)} - 2T_n + T_{(n-1)})/(dx^2) \quad (10)$$

By substituting equation (8) to (10) into equation (1) to (5), the five numerical simultaneous equation were obtained will be as follows;

$$(h_{rgs} + h_{cga} + h_{cgf1} + h_{rpg} + (mc/dt_g))T_{gnm} + (- h_{cf1})\, T_{f1nm} + (-h_{rpg})T_{pnm} = S_1 + h_{rgs}\, T_s + h_{cga}T_a + mc/dt_g T_{gn(m-1)} \quad (11)$$

$$(-h_{cgf1})T_{gnm} + (h_{cgf1} + h_{cpf1} + (m_{ft}c/(wdx)) + (mc/dt_{f1}))T_{f1nm} + (-h_{cpf1})T_{pnm} = +(m_{ft}c/(wdx))T_{f1\,(n-1)\,m} + (mc/dt_{f1})T_{f1n\,(m-1)} \quad (12)$$

$$(-h_{rpg})T_{gnm} + (-h_{cpf1})\, T_{f1nm} + (h_{rpg} + h_{cpf1} + h_{cpf2} + h_{rpb} + (mc_p/dt) - 2(k_p\delta_p)/dx^2)T_{pnm} + (-h_{cpf2})T_{f2nm} - h_{rpb}T_{bnm} = S_2 + (mc_p/dt)T_{p\,n\,(m-1)} - (k_p\delta_p)/dx^2\, T_{p(n-1)m} - (k_p\delta_p)/dx^2\, T_{p(n+1)m} \quad (13)$$

$$(-h_{cpf2})T_{pnm} + (h_{cpf2} + h_{cbf2} + (m_{ft2}c/(wdx) + (mc_{f2}/dt))T_{f2nm} + (-h_{cbf2})T_{bnm} = +(m_{ft2}c/(wdx)T_{f2\,(n+1)\,m} + (mc_{f2}/dt_{f2})\, T_{n\,(m-1)} \quad (14)$$

$$(-h_{rpb})T_{pnm} + (-h_{cbf2})T_{f2nm} + (U_b + h_{cbf2} + h_{rpb} + (mc_b/dt) - 2(k_b\delta_b)/dx^2)T_{bnm} = U_bT_a + (mc_b/dt_b)\, T_{n\,(m-1)}) - (k_b\delta_b)/dx^2T_{b(n-1)m} - (k_b\delta_b)/dx^2T_{b(n+1)m} \quad (15)$$

Several boundary conditions should be identified to solve those five simultaneous equations. Those boundary conditions are listed below;

For $t=0$; $T=T_a$ (16)

For $x=0$;

$$(dT_g/dx) = (dT_p/dx) = (dT_b/dx) = 0;\ T_{f1}=T_i; \quad (17)$$

For $x=L$,

$$(dT_g/dx) = (dT_p/dx) = (dT_b/dx) = 0;\ T_{f2} = T_{f1}; \quad (18)$$

4 Heat Transfer Coefficients

Radiation and convection heat transfer coefficients should be known in order to solve those five numerical simultaneous equations. Radiation heat transfer coefficient is a function of the surface temperature of both sides, while convection heat transfer coefficient is a function of the dimensionless parameter known as Nusselt number (Nu):

$$h_{r12} = \frac{\sigma\left(T_2^2 + T_1^2\right)\left(T_2 + T_1\right)}{\left(\frac{1}{\varepsilon_2} + \frac{1}{\varepsilon_1} - 1\right)} \quad (19)$$

$$h_{c12} = \frac{NuK}{D} \quad (20)$$

Sukhatme [10] and Mohamad [3] had used simple equation to calculate Nusselt number Nu, while Ong [7] give a detailed equations as follow;

For laminar flows (Re<2300);

$$Nu = Nu_\phi + \frac{a\left[\text{Re Pr}\left(D_h/L\right)^m\right]}{1 + b\left[\text{Re Pr}\left(D_h/L\right)^n\right]} \quad (21)$$

For transition region (2300<Re<6000);

$$Nu=0.116(Re^{2/3}-125)Pr^{1/3} \times [1+ (D_h/L)^{2/3}](\mu/\mu_w)\ 0.14 \quad (22)$$

For turbulent region (Re>6000);

$$Nu = 0.036Re^{0.8}Pr^{1/3}\,(D_h/L)^{\ 0.055} \quad (23)$$

Where the constants values are: a=0.0019, b=0.00563, m=1.71, n=1.17, Nu_ϕ =5.4 (Pr=0.7)

Prandtl number Pr given as;

$$\Pr = \frac{\mu c}{k} \quad (24)$$

There is a heat loss from glass cover by radiation to the sky and convection to the ambient air. Sky temperature and radiation heat transfer coefficient are given in equation (25) and (26) respectively:

$$T_s = T_a - 6 \quad (25)$$

$$h_{rgs} = \sigma\varepsilon_g(T_g^2+T_s^2)(T_g+T_s) \quad (26)$$

McAdams [11] has investigated convection heat transfer coefficient into ambient air. Convection heat transfer coefficient from glass into ambient air can be calculated as follows;

$$h_{cga} = 2.8 + 3.8v \qquad (27)$$

Porous media inside the second channel will increase the heat transfer. Mass of porous media m_m depends to the porosity of the media given as below;

$$m_m = (1-\phi)\rho_m\, w d_2 dx \qquad (28)$$

$$\phi = (V - V_m)/V \qquad (29)$$

Hydraulic diameter and Nuselt number for rectangular duct with porous media given as follow (Supranto 2000), (Choudhury & Garg (1993)

$$D_h = \phi \frac{4A}{l} = \phi \frac{2(w)(H)}{(w+H)} \qquad (30)$$

$$Nu = (0.255/\phi)\, Pr^{1/3} Re^{2/3} \qquad (31)$$

5 Computer Programme

The radiation heat transfer coefficient can be calculated after the temperatures distribution inside the system is obtained. While the temperatures distribution in the system can be obtained after the radiation heat transfer coefficient is known. In this case, the temperature inside the systems are initially assumed and specified. Heat transfer coefficients are then evaluated according to the initially-assumed temperature values. The newly calculated temperature values are then compared with the previously assumed values. The iterative process repeated until the difference between the consecutive temperatures is less then 0.1^oC.

6 Experimental Set Up

Double pass solar air heater essentially consists of packed bed duct having a length of 2.4m and a width of 1.2m. The height for the fist channel and second channel are varied. 3kg steel wool was used as porous media in the second channel. Copper-constantan thermocouples were fixed a long the collector at different section to measure temperature distribution such as along the glass cover, the upper air channel, the absorber plate, the lover air channel and the bottom plate. The collector was tested using calibrated solar simulator. A 2.5kW calibrated centrifugal blower has been employed for air circulation in the collector. The temperatures were recorded every five minutes.

The following values of physical parameters have been used;

L=2.4m, w=1.2m, d_1=7cm, d_2=7cm, m_g=5.5kg, c_g=840J/kg/K, α_g=0.06, τ_g=0.90, s_g=3mm, m_p=6.5kg, c_p=500J/kg/K, α_p=0.95, s_g=0.4mm, k_p=237Wm^{-2}, k_b=116Wm^{-2}, m_{f1}=m_{f2}=0.0833 kg/s, c_f=1012J/kg/K, k= 0.0263Wm^{-2}, S=656W/m^2, T_i=T_a=31^{o}C, ϕ=99.92%.

7 Result and Discussion

Theoretical and experimental of temperatures distributions at the different periods of time for air in the first channel are shown in figure 2 and 3, respectively. The temperature at other parts of the collector which is recorded after the steady condition is obtained, which is usually around 40 minute after running the system. These temperatures are shown in figure 4 and 5, as seen from the figures the comparison of the predicted and the experimental temperature results at other parts of the collector shows a good agreement.

The outlet temperature would change with time if input parameters are changing. Figure 6 shows theoretical effects of change solar radiation on outlet air temperature. It found that if the system is running at a solar radiation of 656Wm^{-2}, for 30 minutes and then it drop to 205Wm^{-2}, then the temperature will decline exponentially from around 45^{o}C to 35^{o}C. This model can be used to predict temperature distribution inside the collector by changing the any parameter.

ISSN: 1790-2769

ISBN: 978-960-474-027-7

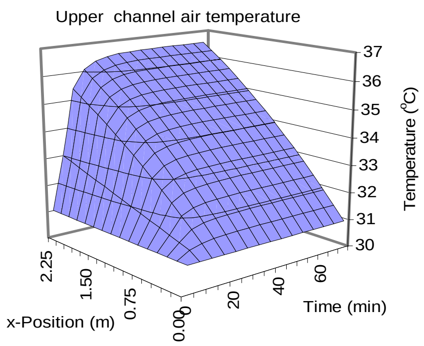

Figure 2: Predicted temperature profile of upper channel air.

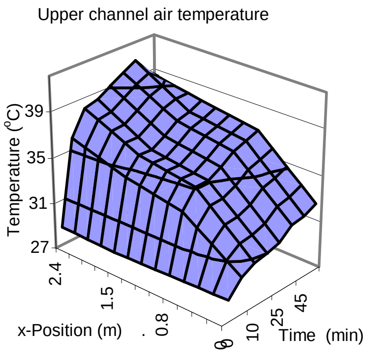

Figure 3: Temperature measurement value of upper channel air

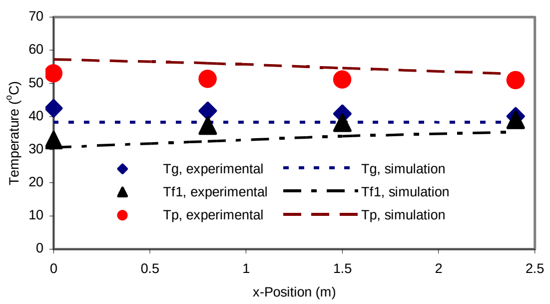

Figure 4: Comparison between predicted and experimental glass cover, upper channel air, and absorber plate temperatures (Tg, T_{f1}, and Tp) after the steady condition is obtained.

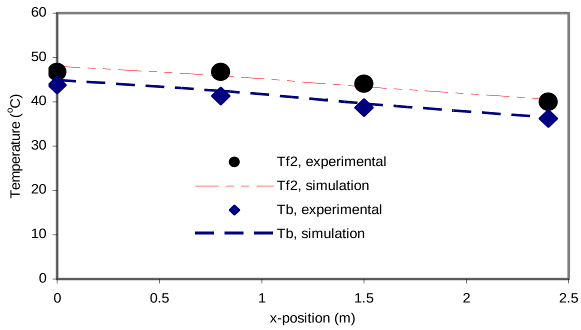

Figure 5: Comparison between predicted and experimental lower channel air and bottom temperatures (T_{f2}, and Tb) after the steady condition is obtained.

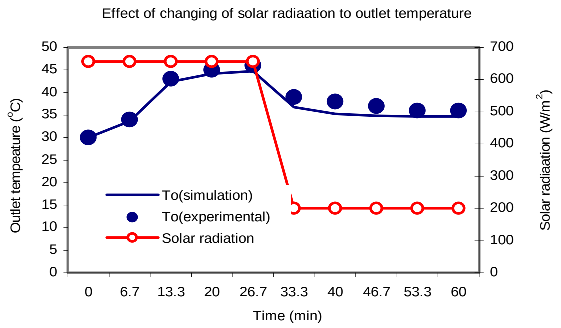

Figure 6: Effect of changing solar radiation to outlet air temperature.

8 Conclusions

Satisfactory quantitative and quantitative agreement was obtained. This model could be use to predict temperature condition in collector in variation of input. The further study of Nusetl number especially in porous media would help the better theoretical result.

Nomenclature

A	Area (m^2)
c	Specific heat capacity (J/kg/K)
D	diameter (m)
d	Height (m)
H	high of the conduct (m)
h	heat transfer coefficient ($W/m^2/K$)
K	heat conductivity (W/m/K)
L	length (m)
M	Mass (kg)
Nu	Nusselt number
P	power (watt)
Pr	Prandlt number
Re	Reynolds number

S solar radiation (W/m^2)
T temperature (^oC)
t time (min)
U heat loss factor (W/m/K)
V volume (m^3)
x thickness (m)
W wide of collector (m)
α absorptivity
δ thickness
τ transmittance
σ Stephen's Boltzmann constant (W/m^2K^4)
ε emissivity
η efficiency
ρ density
μ kinematics viscosity
ϕ porosity

Subscripts
a ambient
b bottom
c convective
f1 upper channel fluid
f2 lower channel fluid
g glass
h hydraulic
nt time interval counter
nx x-position interval counter
o output
p absorber plate
q porous media
r radiative
s sky
w wind

References

[1] Satchunanathan. S, Deonarine. S. A two pass solar air heater. *Solar Energy*, 1975; 15:41-9.

[2] Satchunanathan. S, Persad. P. Experimental evaluation of the multipass solar air heater. In: *Proceedings of the third Miami International Conference on Alternative Energy Sources*, Miami Beach, 1980. p. 375-82.

[3] Mohamad, A.A. High efficiency solar air heater, *Solar Energy*, 1997; 60, 2, 71-76.

[4] Supranto. Reka bentuk dan penilaian sistem pengeringan terbantu suria dua laluan dengan media berliang, *Phd Thesis*, UKM'sia, (2000).

[5] Elradi. A. M. Transient analysis for double-pass solar collector with porous media, *MSc Thesis*, UKM'sia, (2001).

[6] Ooi Eng Hong. Kajian simulasi rekabentuk pengumpul suria dua laluan bermedia berliang dalam sistem pengeringan; *Msc Thesis*; USM, (2002).

[7] Ong. K.S. Thermal Performance of Solar air heater-experimental correlation, *Solar Energy*, 1995, Vol. 55, No. 3.

[8] Sopian. K, Supranto, Daud W. R, Yatim B, Othman M.Y. Thermal performance of double-pass solar collector with and without porous media, *Renewable Energy*, 1999,18/4, 557-564.

[9] Garg. H.P, Sharma B.B, Hargava A.K. Experimental study and theoretical modelling of solar air heater for agriculture use; *Solar World Forum;* 1982, Edited by David O.H and June Morton; UK.

[10] McAdam. W.H. *Heat Transmission*, 3rd ed, 1954; McGraw Hill; New York.

[11] Sukhatme. S.P. *Principles of thermal collection and storage*; Second edition, 1984, McGraw-Hill; New Delhi.